The long-term growth of volcanic edifices: numerical modelling of the role of dyke intrusion and lava-flow emplacement

C. Annen[a,1,*], J.-F. Lénat[b,2], A. Provost[b,3]

[a]Université de Genève, Département de Minéralogie, 13 rue des Maraîchers, 1211 Geneva 4, Switzerland
[b]Université Blaise Pascal and CNRS, OPGC — Laboratoire Magmas et Volcans, 5 rue Kessler, 63038 Clermont-Ferrand Cedex, France

Abstract

The contribution of intrusive complexes to volcano growth is attested by field observations and by the monitoring of active volcanoes. We used numerical simulations to quantitatively estimate the relative contributions to volcano growth of elastic dislocations related to dyke intrusions and of the accumulation of lava flows. The ground uplift induced by dyke intrusions was calculated with the equations of Okada (Bull. Seismol. Soc. Am., 75 (1985) 1135). The spreading of lava flows was simulated as the flow of a Bingham fluid.

With realistic parameters for dyke statistics and lava-flow rheology we find the contribution of dyke intrusions to the growth of a basaltic shield archetype to be about 13% in terms of volume and 30% in terms of height. The result is strongly dependent on the proportion of dykes reaching the surface to feed a lava flow. Systematic testing of the model indicates that edifices tend to be high and steep if dykes are thick and high, issued from a small and shallow magma chamber, and if they feed lava flows of high yield strength.

The simulation was applied to Ko'olau (O'ahu Is., Hawai'i) and Piton de la Fournaise (Réunion Is.) volcanoes. The simulation of Ko'olau with dyke parameters as described by Walker (Geology, 14 (1986) 310; U.S. Geol. Surv. Prof. Pap., 1350 (1987) 961) and with lava-flow characteristics collected at Kilauea volcano (Hawai'i Is.) results in an edifice morphology very close to that of the real volcano. The best fit model of the Piton de la Fournaise central cone, with its steep slope and E–W elongation, is obtained by the intrusion of 10 000 short and thick dykes issued from a very small and shallow magma chamber and feeding only 700 low-volume lava flows. The same method may be applied to the growth of basaltic shields and other volcano types in different environments, including non-terrestrial volcanism. © 2001 Elsevier Science B.V. All rights reserved.

Keywords: volcanic edifices; dyke intrusion; lava-flow emplacement; volcano growth

* Corresponding author. Present address: Department of Earth Sciences, University of Bristol, Wills Memorial Building, Queens Road, Bristol BS8 1RJ, UK. Tel.: +44-117-954-52-43; fax: +44-117-925-33-85.

E-mail addresses: c.j.annen@bristol.ac.uk (C. Annen), j.f.lenat@opgc.univ-bpclermont.fr (J.-F. Lénat), a.provost@opgc.univ-bpclermont.fr (A. Provost).

[1] Tel.: +41-22-702-66-48; fax: +41-22-320-57-32. E-mail: annen@sc2a.unige.ch.
[2] Tel.: +33-473-34-67-46; fax: +33-473-34-67-44.
[3] Tel.: +33-473-34-67-45; fax: +33-473-34-67-44.

1. Introduction

Volcanoes grow through endogenous and exogenous processes, the latter being more conspicuous with the emplacement of volcanic material to surface during eruptions. Clues of endogenous growth, however, are provided by direct and indirect observations. Complexes of thousands of dykes have been observed forming the core of volcanic edifices denuded by erosion or landslides (Walker, 1986, 1987, 1988,
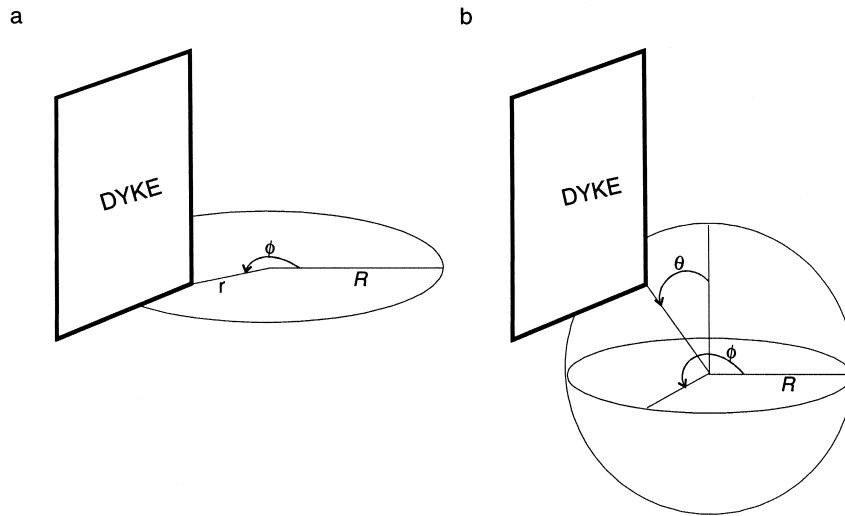
Fig. 1. (a) Disc (penny-shaped) source: the origin of a dyke is defined by its polar angle ϕ (between 0 and 2π) and radial distance r (between 0 and R, the source radius). (b) Spherical source: the origin of a dyke is defined by its longitude ϕ (between 0 and $\pi/2$) and colatitude θ (between 0 and π).

1992, 1999; Takada, 1988; Walker and Eyre, 1995; Walker et al., 1995; Grasso and Bachèlery, 1995; Maillot, 1999). Some persistently active volcanoes release large amounts of gas and heat while emitting proportionally small amounts of lava (e.g. Stromboli volcano, Italy). Their thermal and gas fluxes imply that large, sometimes predominant, amounts of magma are being emplaced in the edifice interior as intrusions or cumulates (Giberti et al., 1992; Francis et al., 1993; Harris and Stevenson, 1997). Geodetic and seismic monitoring of active volcanoes like Kilauea (Hawai'i Is.) and Piton de la Fournaise (Réunion Is.) show that successive intrusions deform and uplift these edifices (Swanson et al., 1976; Decker, 1987; Lénat and Bachèlery, 1990).

Exactly how a volcanic edifice responds to magma intrusion is not clear. Inflation and deflation of a volcano in response to magma chamber filling and draining are well modelled by the theory of linear elasticity (e.g. Mogi, 1958). However, accumulation of the elastic stresses generated by several hundred dykes, not to say thousands, would soon exceed the rock strength and pull the edifice down. The solution of this paradox may rest with the viscoelastic or Maxwell-body (e.g. Middleton and Wilcock, 1994) rheology of the fractured rocks that gradually accumulate to form a volcanic edifice: the short-

term stresses are related to strains through the elastic equations, but the long-term deviatoric stresses are relaxed with only minor large-scale deformation. Such relaxation was measured in NE Iceland following the dyke emplacement into the Krafla volcanic system in 1975–1984 (Foulger et al., 1992), and modelling indicates a relaxation time of only 1.7 years (Hofton and Foulger, 1996a,b). In the present paper we do not investigate the long-term evolution of stresses and potential edifice failure; in the context of a rheological model this amounts to considering that stress decay time is small compared with the characteristic time interval between two neighbouring intrusions.

The aim of our study is to quantitatively appraise the contributions of dyke intrusions and lava flows, respectively, to the growth of basaltic volcanoes. As a first step we compute the ground displacement induced by a swarm of dykes and study the relationships between the source (magma chamber) and dyke geometry and the geometry of the deformation. Next, we simulate the building up of a volcanic edifice by lava-flow accumulation and we study the role of lava-flow parameters. Finally, we merge the two approaches to model simultaneously the endogenous and surface growths and we investigate the respective contributions of the two processes according to
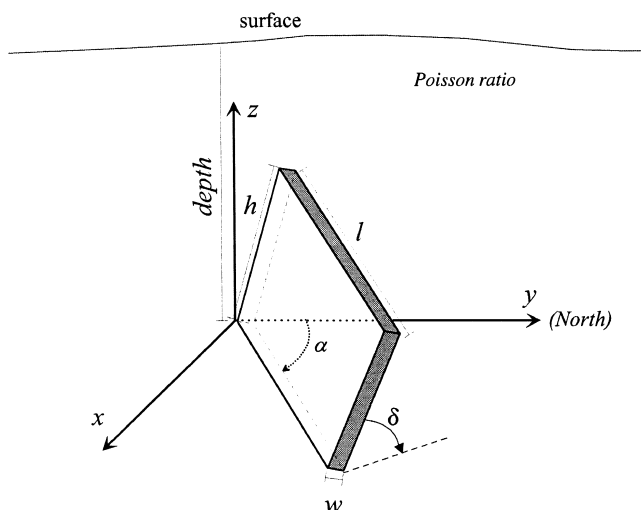
Fig. 2. We model dykes as parallelepipeds described by their length l, height h, width w, dip δ and azimuth α, along with the co-ordinates of their origin (Fig. 1). Axes Ox and Oy are oriented east and north, respectively. The medium is characterised by its Poisson ratio ν.

different situations. The simulation is applied to the growth of Ko'olau volcano (O'ahu Is., Hawai'i) and Piton de la Fournaise.

2. Endogenous growth by dyke intrusions

2.1. The model

We assume that the displacements induced by the intrusion of a dyke are equivalent to those associated with the opening of a tensile fault (Okada, 1985; Yang and Davis, 1986). The ground displacement is calculated using the equations of Okada (1985) for parallelepiped-shaped tensile faults in a homogeneous elastic half-space. Sophisticated models are now available for particular or more realistic conditions like a shallow dyke tip (Bonafede and Danesi, 1997) or a layered elastic medium (Bonafede and Rivalta, 1998), but such complications are not warranted for this first-order, statistical approach. As we do not investigate the stresses but just calculate ground displacements from dyke openings, the only material characteristic needed is the Poisson ratio of the volcanic edifice.

We assume that dykes are injected from the upper half of a magma reservoir, and consider three possible shapes for the reservoir: point, disc and sphere. A point source represents a reservoir that is very small compared to its depth z_S, or a small area of a magma chamber where tensile stresses are concentrated. A disc (penny-shaped) source may represent a magma sill or a fully three-dimensional reservoir with a flat roof. A spherical source approximates a reservoir with a highly curved roof. The origin of a dyke is fixed in the case of a point source but otherwise it is defined by two parameters: polar angle ϕ and radial distance r for a disc source (Fig. 1a), longitude ϕ and colatitude θ for a spherical source (Fig. 1b).

The spatial distribution of dyke origins depends on the distribution of tensile strength across the reservoir surface, which itself depends on reservoir geometry and depth, loading conditions and regional stress field, mechanical structure of the edifice and elastic properties, etc. (Gudmundsson, 1998). For this simple study we assume that the distribution of dyke origins is spatially uniform, i.e. that its density of spatial probability is a constant (per unit area). For a disc or spherical source this means that ϕ and r^2 (disc) or ϕ and $\cos\theta$ (sphere) are taken as uniformly distributed.

The dimensions and orientation of a dyke are defined by its length l, height h, width w, azimuth (strike) α and dip δ (Fig. 2). These dyke characteristics are random variables for which we consider only simple, two-parameter statistical laws: uniform, positive-Gaussian,

Table 1
Mean width and standard deviation of width in outcropping dyke complexes

Dyke swarm	Mean width (cm)	Standard deviation (cm)
Alofau volcano (Walker and Eyre, 1995)	40.4	40.2
Pago volcano (Walker and Eyre, 1995)	46.4	41.2
Ofu-Olosega volcano (Walker and Eyre, 1995)	50.8	36.4
Piton des Neiges volcano (Maillot, 1999), basaltic dykes only	56.0	51.1
Ko'olau volcano (Walker, 1987)	74.5	48.4
Piton des Neiges volcano (Maillot, 1999), all dykes	78.5	215
Piton de la Fournaise volcano (Grasso and Bachèlery, 1995)	98.1	74.4
Hvalfjördur volcano (Gudmundsson, 1995a)	109	143
Mt Etna (Compare, 1980)	174	138
Eastern Iceland regional dykes (Gudmundsson, 1990)	348	371
Flateyjarskagi peninsula (Gudmundsson, 1995a)	535	531

log-normal, truncated exponential and truncated power-law (see Appendix A). Actually, the statistical distributions of dyke characteristics are probably not independent, e.g. long dykes are expected to be higher and thicker than short dykes, on average. Multidimensional distributions could easily be introduced into our program but we did not consider it useful at this stage for the following reasons: (1) realistic multidimensional distributions for the various dyke parameters are not presently available and no statistical study of parameter correlations has yet been carried out; (2) a systematic study of the influence of parameter correlations would be rather clumsy and inappropriate to this preliminary study; (3) with regard to dyke dimensions what really matters for the morphology of a volcano is the accumulated width of dykes as a function of depth, radial distance and polar angle (many thin dykes have the same effect as a few thick dykes), the results are not too sensitive to the statistical details of how the final structure has been obtained.

Our tests simulate the emplacement of a large number of dykes. A single simulation run requires one to select the Poisson ratio value, the geometry and depth of the magma reservoir, a statistical law for each of the five dyke dimension and orientation characteristics, the parameters of each law, and the number of dykes. For every intrusion the vertical and horizontal components of ground displacement are computed at the nodes of a rectangular grid and accumulated for the whole set of dykes. The result is a digital elevation model.

2.2. Model parameters: the geological and geophysical evidence

Input data were based on field observations and geophysical measurements reported in the literature. Data sets large enough to have statistical value are reported for the dyke widths, strikes and/or dips of Mt Etna (Compare, 1980), Ko'olau volcano (Walker, 1987), Samoan Islands (Walker and Eyre 1995; Walker et al., 1995), Iceland (Gudmundsson, 1983, 1990, 1995a,b, 1998) and Réunion Island (Grasso and Bachèlery, 1995; Maillot, 1999). Most data sets, however, are only available in the form of histograms with classes of uniform size. Though classical, this presentation represents a severe loss of information, especially when a few classes are numerically dominant as is often the case for dyke width (low values) and dip (values close to 90°). Histograms can nevertheless be used to approximately reconstruct the cumulative probability functions and compare them to the prediction of various statistical laws, either quantitatively through least-squares modelling or qualitatively through the use of appropriate probability diagrams (e.g. Walker and Eyre, 1995).

The best-documented characteristic of dykes is their width. A quantitative analysis of all published dyke statistics has not been completed yet but the preliminary results are interesting. They concern Mt Etna (Compare, 1980), Ko'olau volcano (Walker, 1987), Hvalfjördur volcano, Western Iceland (Gudmundsson, 1995a), Flateyjarskagi Peninsula,

Table 2

Width, height and depth (from earth surface to dyke top) of Kilauea dykes (Hawai'i Is.), estimated from geophysical monitoring

	August 1968[a]	May 1970[b]	September 1971[b]	August 1981[b]	1971–1983[c]
Width (m)		0.8	1.6		
Height (m)		400	3800	3000	2000–3000
Depth (m)	140	400	0	250	

[a] Jackson et al. (1975).
[b] Pollard et al. (1983).
[c] Dvorak and Okamura (1987).

Northern Iceland (Gudmundsson, 1995a), Eastern Iceland regional dyke swarms (Gudmundsson, 1990), Piton de la Fournaise volcano (Grasso and Bachèlery, 1995), Piton des Neiges volcano (Maillot, 1999) and the Samoan volcanoes Pago, Ofu-Olosega and Alofau (Walker and Eyre, 1995). The fashionable power-law statistics (e.g. Grasso and Bachèlery, 1995; Gudmundsson, 1995a,b, 1998) give the best fit in only one case (Alofau) and give a very bad fit for the other nine data sets. For some data sets they give a relatively correct fit (though worse than other laws) if a few classes are eliminated at one or both ends of the thickness spectrum. This illustrates the danger of speculating about a distribution law based on the visual inspection of histograms or even a probability diagram when only one statistical law is considered. The log-normal fit is bad for only two data sets (Flateyjarskagi and Alofau), runs from fair to excellent for the other eight and gives the best fit for seven data sets. For Flateyjarskagi the best fit is given by the positive-Gaussian law; this law ties for the first place with the log-normal fit for Ko'olau but gives very bad, bad or just fair fits for the other eight. The exponential law gives a bad fit for four data sets, a fair fit for another four, and a good (best and second-best) fit for the Eastern Iceland regional dykes and Pago. Of course the uniform distribution is never appropriate for dyke width. The mean width $\bar{w}$ of these ten dyke swarms (Table 1) varies from 40 cm (Alofau) to 5.4 m (Flateyjarskagi). The standard deviation σ_w is often comparable with the mean yet the $\sigma_w/\bar{w}$ ratio varies from 0.65 (Ko'olau) to 2.7 (Piton des Neiges).

The statistical analysis of dyke dips and strikes has not yet been done. Dip histograms at Kilauea, Pago-Alofau and Flateyjarskagi are asymmetrical (log-normal-looking) with modes between 75 and 85°. Most Tertiary dykes in Iceland are subvertical (Gudmundsson, 1990); their histograms, with modes between 85 and 90°, are exponential-looking but this does not preclude that another distribution law (including log-normal) could give the best fit. At Hvalfjördur the dip and strike histograms are bimodal, possibly indicating the superposition of two different dyke populations. Other strike histograms are symmetrical (Gaussian-looking) or slightly asymmetrical, or bimodal, looking like the superposition of two broadly symmetrical distributions. Of course the classical statistical laws are not well adapted to dip and strike statistics because of the definition space (the closed segment $[-90°, 90°]$ for dip and the periodic segment $[0°, 360°]$ for strike).

Very scarce information on dyke length and virtually no information on dyke height have been obtained by direct observation on the field. Only a few dykes have been followed along their length and the measured lengths are presumably minimum values because the lateral ends are not seen (Gudmundsson, 1995b). At Piton de la Fournaise (Grasso and Bachèlery, 1995) the histogram of about 400 fissure lengths ($\bar{l} = 46$ m, $\sigma_l = 38$ m) is well fitted by a log-normal law and cannot result from a power-law or positive-Gaussian distribution. On the Reykjanes Peninsula, SW Iceland (Gudmundsson, 1995b) the length size distribution of 31 Holocene volcanic fissures ($\bar{l} = 2.6$ km, $\sigma_l = 2.2$ km) shows two disjoined populations, one possibly resulting from a log-normal or exponential distribution (not power-law or positive-Gaussian) and the other too small for statistical analysis.

For dyke length and height at least, it is better to rely on geophysical data collected on active volcanoes. For example at Kilauea, the interpretation of geophysical data collected during intrusive episodes (Swanson et al., 1976; Pollard et al., 1983; Dvorak and Okamura, 1987; Decker, 1987) indicates

Table 3
Medium, source and dyke parameters used in the reference model of dyke intrusions (isotropic distribution of azimuths, Section 2.3.1) and its anisotropic variants (Section 2.3.2). A "Gaussian" distribution means a positive-Gaussian law (see Appendix A); for this law the "minimum" and "maximum" values stand for $x_0 - 2s$ and $x_0 + 2s$ (cf. Eq. (A12)). A dip value δ greater than 90° is equivalent to $(180° - \delta)$ dip and $(\alpha \pm 180°)$ azimuth

Characteristics of the medium	Poisson ratio		0.25
Characteristics of the source (sphere or disc)	Depth (m)		2000
	Radius (m)		500
Characteristics of the dykes	Width (m)	Minimum	0.25
		Maximum	0.75
		Distribution	Gaussian
	Length (m)	Minimum	1000
		Maximum	5000
		Distribution	Gaussian
	Height (m)	Minimum	500
		Maximum	3000
		Distribution	Gaussian
	Dip (°)	Minimum	70
		Maximum	110
		Distribution	Uniform
	Azimuth (°) (isotropic)	Minimum	0
		Maximum	360
		Distribution	Uniform
	Azimuth (°) (anisotropic: rift zone 1)	Minimum	80
		Maximum	100
		Distribution	Uniform
	Azimuth (°) (anisotropic: rift zone 2)	Minimum	260
		Maximum	280
		Distribution	Uniform

several-kilometre, vertical or subvertical dykes, 400–3800 m high with thicknesses around 1 m (Table 2). The top and bottom depths of the magma chamber at Kilauea are estimated with the same techniques at 2–3 and 4–7 km, respectively (Jackson et al., 1975; Ryan, 1987; Delaney and McTigue, 1994).

2.3. Results

2.3.1. Isotropic distribution of radial dykes

For a volcano which does not show preferential lateral zones of vents, the development of its dyke complex may be simulated with an isotropic distribution of intrusions beneath the summit. Here we give the result of such a simulation with the intrusion of 5000 dykes issuing from a magma chamber located at 2 km depth. The distribution laws of dyke dimensions and orientation are reported in Table 3. The resulting

deformation builds a cone. Cones obtained from a point or disc source are very similar in shape and size and reach about 265 m in height. For a spherical source the cone is lower (~175 m) and wider and exhibits an apical depression about 25 m deep (Fig. 3).

The influence of the dimensions of the dykes and of the depth and size of the source was systematically examined. For dyke height it must be noticed that the probability law characterises the ability of dykes to make their way through the edifice rocks so the (potential) height can exceed the distance from source to free surface. When the random variable for height gets a value greater than the maximum acceptable value (reservoir depth plus accumulated uprising), it means that the dyke reaches the surface and the dyke height is given this maximum value. The model described above for a spherical source served as a reference model to normalise the results (shown as

Height =178 m   Height = 263 m   Height = 266 m

Spherical source   Disc   Point source
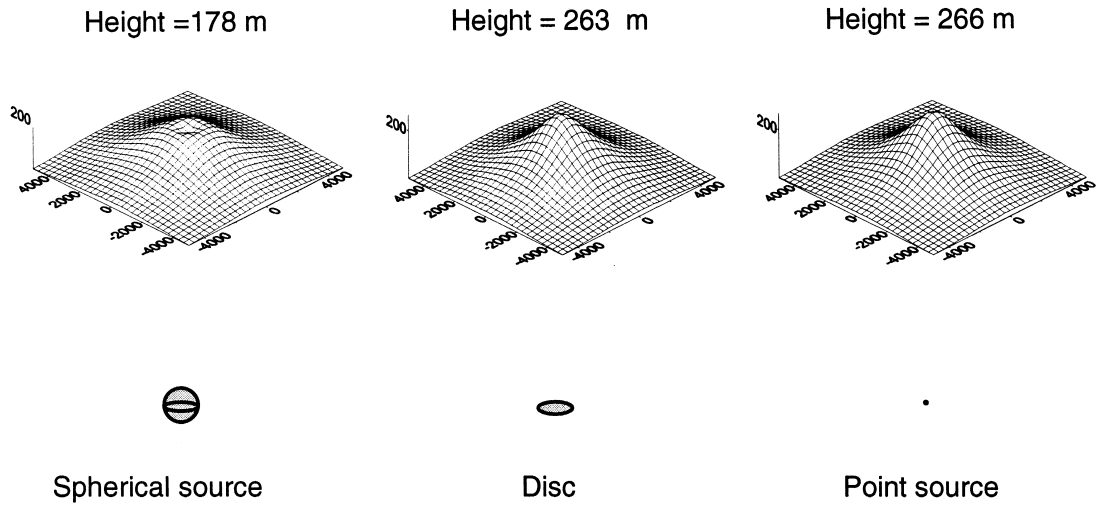
Fig. 3. Perspective view of the deformation induced by the intrusion of 5000 dykes with characteristics as listed in Table 3, with a spherical source, a disc source or a point source. Graduations in metres, vertical exaggeration: 13 ×.
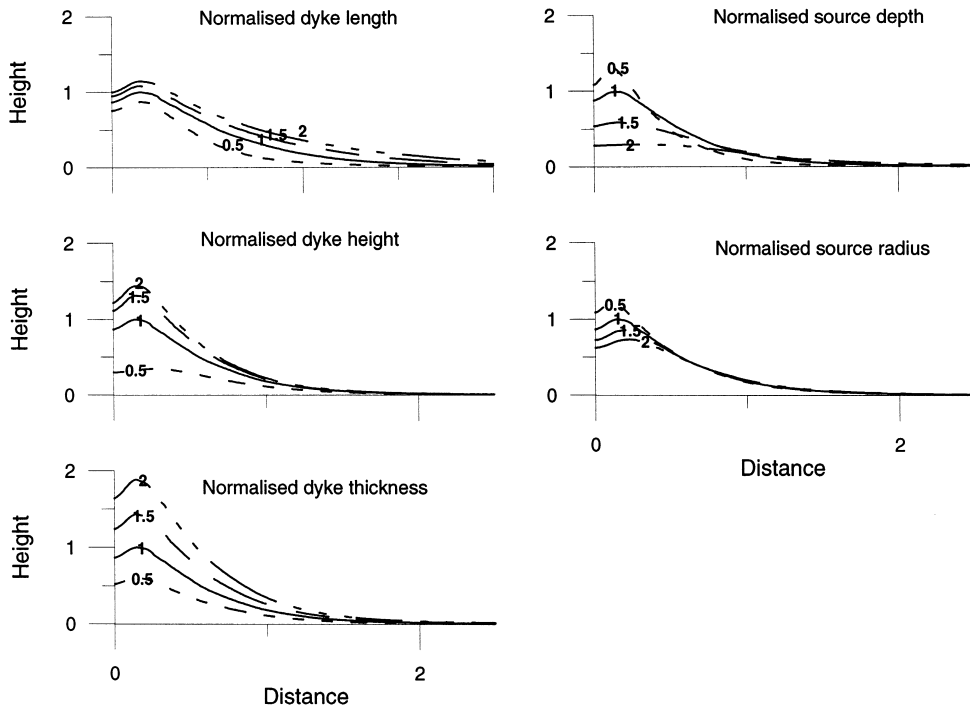

Fig. 4. Half profiles of the deformation induced by 5000 dykes issuing from a spherical source using different mean values of dyke length, height and thickness, and of source depth and radius. The values of dyke and source parameters are normalised to the corresponding parameter of the reference model. The horizontal distance (abscissa) and deformation height (ordinate) are normalised to the half-width and maximal height of the reference model, respectively.
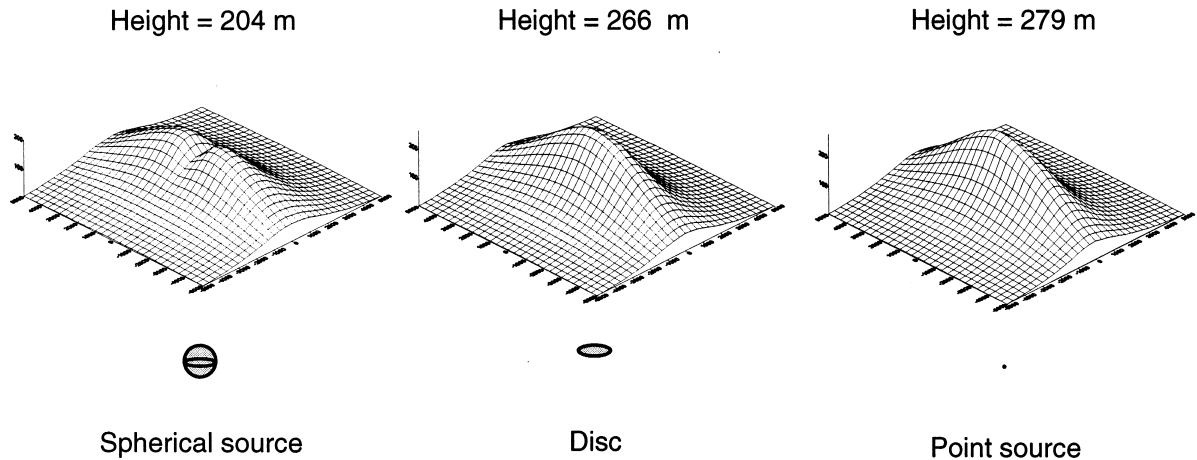
Height = 204 m   Height = 266 m   Height = 279 m

Spherical source   Disc   Point source

Fig. 5. Perspective view of the deformation induced by 5000 dykes preferentially oriented along two directions at 180°, with a spherical source, a disc source or a point source. The model parameters are listed in Table 3. Graduations in metres, vertical exaggeration: 13 × .

profiles on Fig. 4). The bulge gets higher and steeper if the thickness and height of the dykes increase and it is wider and flatter if intrusions are longer. With the same intrusive volume, the amplitude of the vertical displacement decreases and the width of the uplifted area increases as the source deepens. An increase in the radius of the reservoir in the case of a spherical or disc source results in a lower and wider swell. The uplift produced with a disc source is significantly different from the one generated with a point source only if the diameter of the disc source is relatively large, more than one third of the depth. A summit depression, always present for a spherical source, appears in the case of a point or disc source if less than 10% of the dykes reach the surface. The ratio of the volume of the bulge to the intruded volume remains practically constant and is approximately 2/3 for a Poisson ratio of 0.25 (in fact, it decreases slightly when the depth of the source increases or the height of the dykes decreases).

In this section the distribution of dyke strikes was taken as uniform over $[0°, 360°]$. For the other dyke characteristics the uniform law is not realistic but any of the four other distribution laws (positive-Gaussian, log-normal, truncated exponential and power law) could be reasonably chosen. We did not check all the possible combinations but, starting from the reference model of Table 3, we investigated the effect of changing the distribution law for a given dyke characteristic while keeping the same mean and standard deviation. For all dyke characteristics but height, the effect on the quantitative results is of the order of 10% and does not pass beyond 15%. For dyke height it reaches values of 30–40%. In particular the truncated exponential and power laws give a smaller swelling with a more pronounced apical depression; this may be due to the fact that these distribution laws give a lower proportion of shallow dykes. Though significant, the effect of changing the shape of a distribution law is much less than that of changing the mean and standard deviation so most numerical tests were done with the positive-Gaussian law for each dyke characteristic except strike. For width, length and height the log-normal law would have been more realistic but the parameters of the positive-Gaussian are more readily understood in physical terms, without affecting the quantitative results too much.

2.3.2. Anisotropic dyke complexes: the rift-zone case

Most shield volcanoes have rift zones extending from the summit. Commonly, there are two main volcanic rift zones on basaltic shields (e.g. Kilauea and Mauna-Loa, Hawai'i Is.; Piton de la Fournaise, Réunion Is.); sometimes three well-developed rift
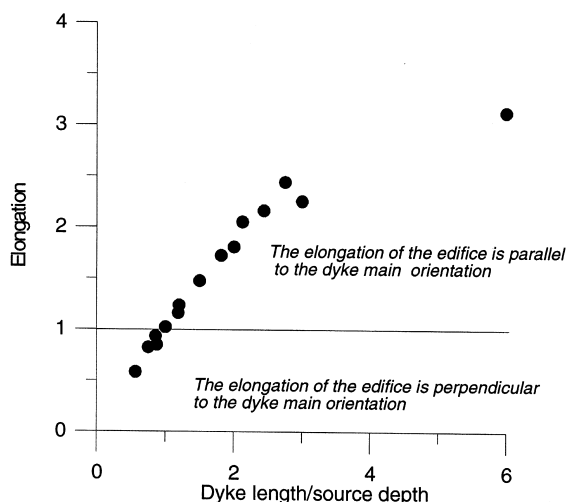
Fig. 6. Bulge elongation e (Eq. (1)) induced by preferentially oriented dykes, versus the ratio of mean dyke length to source depth; $e > 1$ if the edifice is elongated parallel to the preferred orientation of dykes and $e < 1$ if it is elongated perpendicularly.

zones are present (e.g. Hierro and possibly Tenerife, Canary Islands). Here we consider the case with two symmetric rift zones at 180°. The preferential emplacement of dykes in rift zones is simulated by imposing constraints to the distribution of dyke azimuths.

The main difference from the isotropic case is that the bulge is now elongated. For the typical parameters of Table 3 it is elongated parallel to the rift zones, and in the case of a spherical source the ridge is cut perpendicularly by a summit valley (Fig. 5). Bulge elongation may be defined quantitatively as:

$$e = \frac{L}{W} \tag{1}$$

where L is the length of the bulge in the direction parallel to the average orientation of dykes and W is its width in the perpendicular direction: if $e > 1$ the bulge is elongated in the preferred direction of dykes, if $e < 1$ it is elongated perpendicularly to this preferred direction, and $e = 1$ corresponds to a roughly axisymmetric bulge. Elongation e depends on the mean dyke length over source depth ratio, $\bar{l}/z_S$ (Fig. 6): long dykes favour $e > 1$ while deep sources favour $e < 1$.

3. Surface growth by lava-flow accumulation

3.1. The model

We simulate the exogenous growth of a volcano by an accumulation of lava flows spreading over a grid of square cells. Models like those of Ishihara et al. (1990), Young and Wadge (1990) and Barca et al. (1993) were devoted to the prediction of lava-flow contours as a function of time for a single eruption, in the context of civil defence. They are excessively time-consuming and unnecessarily detailed for our purpose. Our aim is to estimate how hundreds of lava flows contribute to volcano growth; we do not need to know the exact path and morphology of any single flow. What we want is a robust model that respects the basic physics of lava flow and the average relations between the final volume and dimensions of lava flows. We opted for a simple model of a Bingham liquid which follows the steepest slope and spreads laterally according to its rheology. Our model uses the equation of Hulme (1974):

$$h = \frac{\sigma_y}{\rho g \sin \alpha} \tag{2}$$

where h is the flow thickness, σ_y and ρ are the lava yield strength and density, g is gravity and α is the surface slope.

When slope α tends to 0°, the thickness given by Eq. (2) increases indefinitely, which of course is unrealistic. On small slopes the final height of a flow is not governed by the steady-state relation between flow thickness and downslope speed (which leads to Eq. (2) for vanishing speed), but rather by lateral spreading. For a Bingham liquid, lateral spreading ceases when slope of the flow surface is so low that shear stress inside the flow is everywhere less than yield strength σ_y. This results in the following expression for the maximum flow thickness:

$$h(\alpha \leq k) = h_{max} = \frac{\sigma_y}{\rho g k} \tag{3}$$

where k is the aspect ratio of the flow, i.e. the width of the lava flow is given by:

$$w = \frac{h}{k} \tag{4}$$

For each lava flow the vent position, the flow

Table 4
Statistics of the volume, thickness and length of n lava flows at Mt Etna (Italy), Kilauea (Hawai'i Is.), Mauna Loa (Hawai'i Is.) and Piton de la Fournaise (Réunion Is.)

		Volume (10^6 m^3)	Thickness (m)	Length (km)
Etna $n = 39$	Minimum	1.2	2	0.25
	Maximum	1050	50	14
	Median	60	10	7.25
Kilauea $n = 44$	Minimum	0.01		
	Maximum	185		
	Median	7.5		
Mauna Loa $n = 20$	Minimum	3		
	Maximum	460		
	Median	110		
Piton de la Fournaise $n = 82$	Minimum	0.1		
	Maximum	130		
	Median	3		

volume and aspect ratio, and the lava yield strength and density are considered as random variables with given distribution laws. The aspect ratio k, yield strength σ_y and volume V are not fully independent, however, because the width of a flow cannot be larger than its length:

$$\frac{\sigma_y}{\rho g k^2} < \frac{\rho^2 g^2 k^3 V}{\sigma_y^2} \tag{5}$$

where the left side corresponds to the maximum width of the flow and the right side to its minimum length. If a set of parameters does not comply with this constraint a new set is picked until condition (5) is fulfilled.

Lava flows from the vent cell then follows the steepest slope of the volcano. At each newly invaded cell, the program calculates the final thickness and width of the flow with Eqs. (2)–(4). When the calculated width of the flow exceeds that of a cell, the excess lava is assigned to adjacent cells. The flow proceeds from cell to cell downwards, until its volume is exhausted. Edifice topography is then updated before the next flow starts.

3.2. Model parameters: the geological evidence

A numerical simulation must be based on realistic distributions of lava-flow characteristics but the published data are few. Walker (1973) gives the length histograms of 479 low-viscosity (basalt and

mafic feldspathoid-bearing) and 417 high-viscosity (trachyte, andesite and rhyolite) lava flows from various locations. Volume, length and thickness are known for 40 lava flows at Etna (Romano and Sturiale, 1982). Volumes are also available for most historical lava flows at Kilauea (Macdonald et al., 1986, pp. 80–81; HVO, 2000a), Mauna Loa (Lockwood and Lipman, 1987; HVO, 2000b) and Piton de la Fournaise (Bachèlery, 1981; unpublished data from the Observatoire Volcanologique du Piton de la Fournaise). Some of these statistics are reported in Table 4. A large range of average flow volume is observed at different volcanoes, from a median value of 3×10^6 m^3 at Piton de la Fournaise to 1.1×10^8 m^3 at Mauna Loa. The distribution of eruption volumes at Etna may be exponential or positive-Gaussian, at Mauna Loa it may be exponential (or power-law if we neglect the smallest flows), at Kilauea and Piton de la Fournaise it seems to be log-normal. The three data sets for flow length are compatible with a log-normal distribution but the positive-Gaussian law works as well for Etna and the exponential law for Walker's two groups. None of the four distribution laws fits the flow thicknesses at Etna well.

3.3. Results

We simulate the accumulation of 1700 lava flows with characteristics as summarised in Table 5. The number of flows corresponds to the number of dykes

Table 5
Lava-flow parameters used in the reference models for lava-flow accumulation (Section 3.3) and endogenous plus surface growth (Section 4). For the "Gaussian" distribution, see caption of Table 3

Volume (10^6 m^3)	Minimum	10
	Maximum	100
	Distribution	Gaussian
Yield strength (kPa)	Minimum	1
	Maximum	10
	Distribution	Gaussian
Distance from vent to grid centre (m)	Minimum	0
	Maximum	3600
	Distribution	Gaussian
Aspect ratio	Minimum	0.005
	Maximum	0.05
	Distribution	Gaussian

that reach the surface in the reference model for dyke intrusions (cf. Section 2.3.1). The lava flows build a cone 525 m high and 18 km wide with a mean slope of 3° (Fig. 7). This first model serves as a reference for the systematic survey of the influence of each model parameter.

Density is not a crucial parameter because of its small variation range. The final height and shape of the edifice depend mainly on the thicknesses and lengths of the lava flows. Flow thickness is a direct function of the yield strength (Eq. (2)) and flow length is a direct function of lava volume and an inverse function of lava thickness, hence of the yield strength.

In consequence, the height of an edifice built up by lava flows will be a direct function of lava yield strength (Fig. 8). Its slopes will be steep if the yield strength is large and if volumes are small. Another factor with a strong influence on the height and slopes of modelled volcanoes is the distribution of vents. Evenly distributed vents generate a low and flat edifice whereas concentrated vents generate high and steep volcanoes (Fig. 8).

We can simulate rift zones by focusing vents along some direction. The edifice becomes elongated in that direction (Fig. 9). The edifice elongation e (Eq. (1)) depends on the mean distance from vents to the grid centre, but is always greater than 1.

4. The building of volcanoes: endogenous versus surface growth

The final step in our simulation is to merge the two models in such a way that each time a dyke reaches the surface it produces a lava flow. Based on some visual observations at Piton de la Fournaise and Kilauea volcanoes, the position of the vent is fixed at a distance of 2/3 of the dyke length, downstream, on the surface dyke trace. With dyke parameters described in Table 3 and lava-flow parameters described in Table 5, we simulate the intrusion of 5000 dykes. 1669 dykes reach the surface and feed lava flows. The resulting construct is an edifice 510 m high and 16.8 km wide with a mean slope of 3° (Fig. 10).
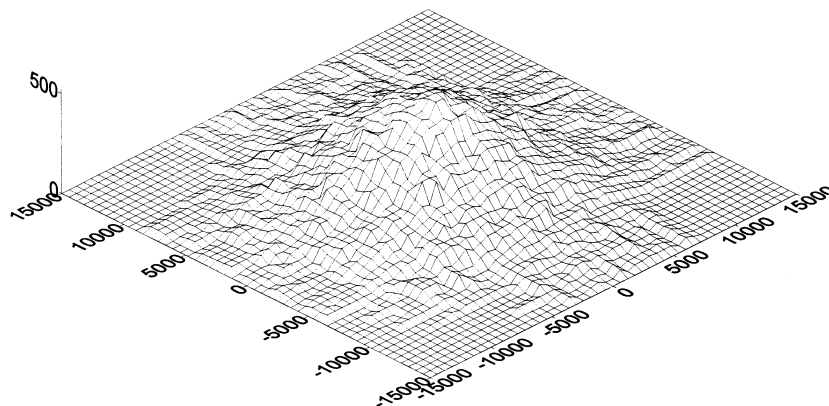

Fig. 7. Perspective view of the edifice built by 1700 lava flows with characteristics as listed in Table 5. Graduations in metres, vertical exaggeration: 13 × .
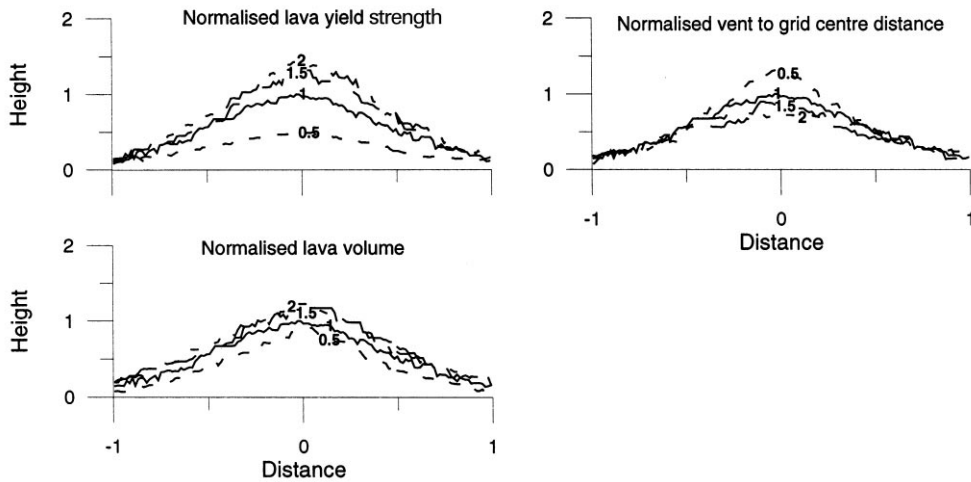
Fig. 8. Normalised profile of the edifice built by the accumulation of 1700 lava flows, for different mean values of lava yield strength, flow volume and vent to grid centre distance. Each parameter is normalised to the corresponding value of the reference model (Table 5). The horizontal distance (abscissa) and edifice height (ordinate) are normalised to the half-width and maximal height of the reference model, respectively.

In addition to their influence on endogenous growth (cf. Section 2.3.1), the intrusion characteristics also determine the occurrence and location of surface lava vents. In particular, the ratio of mean dyke height to source depth controls the number of intrusions that reach the surface. A large range of dyke lengths yields vents scattered over a large surface and results in a wide and flat volcano. The dip of the dykes influences their ability to reach the surface and the location of the vents. High and steep volcanoes are built up by numerous lava flows emitted from vents concentrated in a restricted area and host complexes of high, short and steeply dipping intrusions whereas low and flat volcanoes host complexes of little-height, long and shallow-dipping dykes, all other parameters being equal. The size of the source also influences the distribution of vents: a large magma chamber favours scattered vents and low edifices.

The contribution of dyke intrusions to volcano growth can be expressed in terms of volume or in
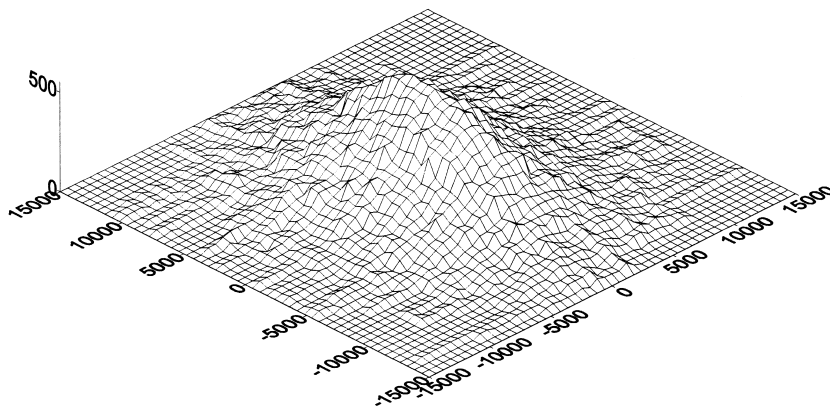

Fig. 9. Perspective view of the edifice built by the accumulation of 1700 lava flows with vents preferentially set out along a line. Graduations in metres, vertical exaggeration: 13 ×.
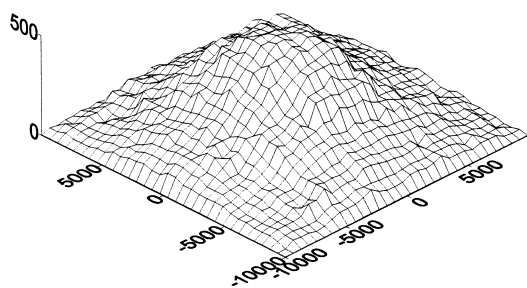
Fig. 10. Perspective view of the edifice built by the intrusion of 5000 dykes (Table 3) feeding 1669 lava flows (Table 5). Graduations in metres, vertical exaggeration: 13 ×.

terms of height. The contribution in terms of height is calculated by comparing the height of the deformation induced by dykes only with the height of the edifice built up by both dyke intrusions and lava-flow accumulation. The contribution in terms of volume is obtained by subtracting the volume of emitted lava from the total volume of the volcano. For the reference model, the contribution of dyke intrusions is 34% in terms of height and 13% in terms of volume. The contribution in terms of volume mainly depends on the intrusion and lava volumes (number and mean volume of dykes, number and mean volume of flows) (Fig. 11a). The contribution in terms of height is related to the geometry of dykes, to lava rheology and also to the number of dykes that feed a lava

flow (Fig. 11b). In the limiting case where no dykes reach the surface, the contribution of dykes to height and volume of the edifice is 100%; in the opposite case where every dyke reaches the surface the contribution of the intrusives is very low (less than 5%) in terms of volume but significantly higher (around 30%) in terms of height (Fig. 11).

5. Case study 1: Ko'olau volcano

Ko'olau (O'ahu Is., Hawai'i) is a two million year old basaltic shield volcano. It is elongated NW–SE and its emerged length is 57 km. It is 960 m high (a.s.l.) but the extrapolation of slopes yields an original elevation of 1100 m above present sea level (Walker, 1987) (Fig. 12). In addition, bathymetry suggests a 500-m subsidence of the island since the end of Ko'olau activity. Thus, Ko'olau volcano may initially have been 1600 m high and 77 km long. The mean slope is around 6°. The flanks have been deeply cut by landslides and erosion, revealing a huge dyke complex forming the core of the edifice.

Walker (1986, 1987) carried out an exhaustive study of this complex. He measured 3500 dykes and estimated the total number of dykes to be at least 7400. Most dykes occur in a major rift zone oriented NW, about 35 km long and with a maximum width of 7 km. A secondary, narrower dyke complex is oriented SW. The dyke intensity (i.e. the percentage
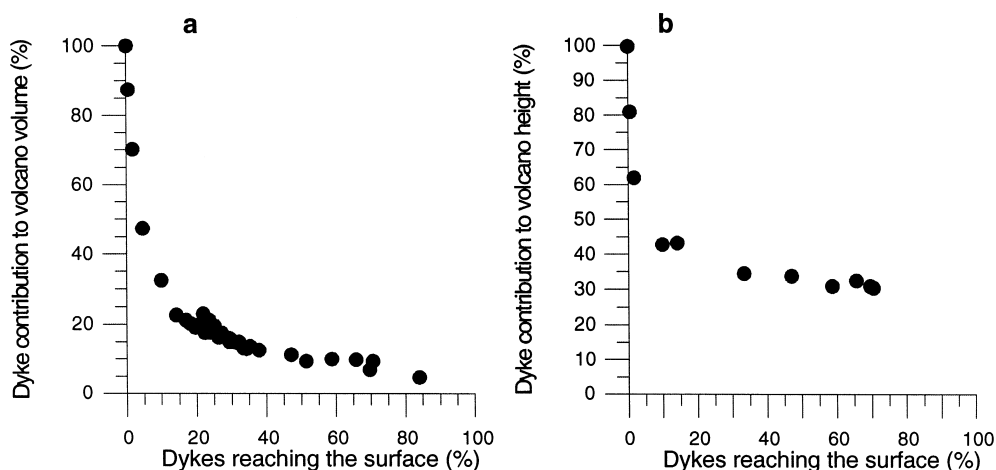

Fig. 11. Contribution of dyke intrusions to volcano growth versus the percentage of dykes reaching the surface: (a) contribution in terms of volume; and (b) contribution in terms of height.
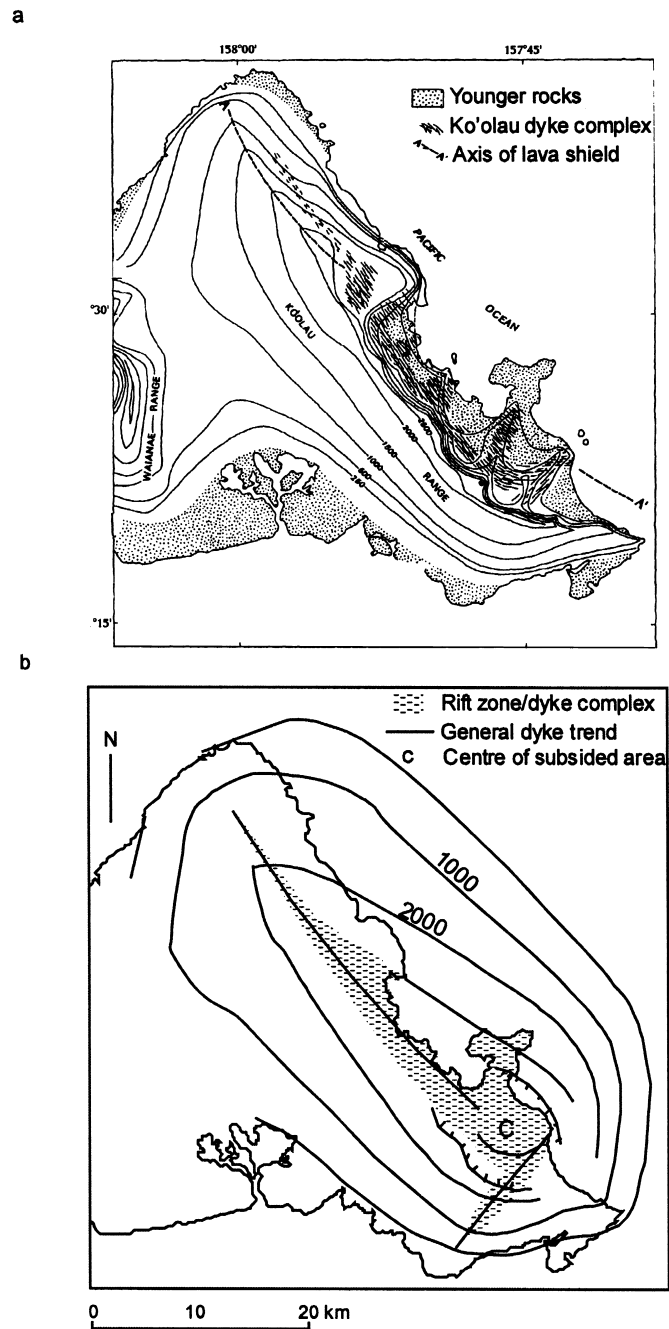
a

b

Fig. 12. (a) Map of present-day Ko'olau volcano (O'ahu Is., Hawai'i) (Walker, 1987). (b) Reconstruction of the original edifice by extrapolating slopes (Walker, 1987); contour labels in feet.
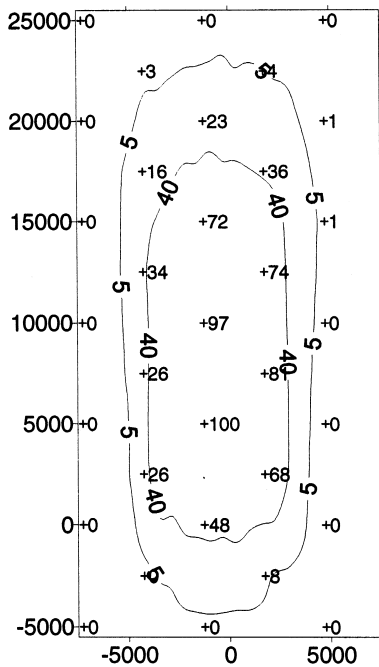
Fig. 13. Map of dyke intensity 1000 m below the initial ground surface, obtained from model Ko'olau2 (intensities in model Ko'olau1 differ by a few percent only). This map compares well with the map constructed by Walker (1987) using field data. Graduations in metres, dyke intensity in %.

of dyke rock versus bedrock) varies little across the rift zone, with an axial part greater than 40% reaching 80% locally and a narrow margin belt of intensity values between 5 and 40%. The width of the dykes follows a log-normal distribution with a median of 65 cm. The intrusions are not vertical but dip from 65 to 85° in conjugate directions (Walker, 1987). Walker (1987) estimated the total vertical displacement induced by the dyke complex at 1000–1500 m, by summing the vertical component of the dislocation vector. However, his approach does not take into account the mechanical properties of the medium.

We simulated the intrusion of 7400 dykes with characteristics constrained by the field observations of Walker (1986, 1987). The intensity map of the model was compared with that of Walker and used to adjust the length and dip parameters of the intrusions, in order to obtain a comparable pattern (Fig. 13). The geometry of the reservoir is not known but the high intensity of intrusions over a 4-km-wide zone suggests that the source zone has the same extension. We chose a depth of 3000 m for the reservoir according to the estimation available for Kilauea volcano (Jackson et al., 1975; Ryan, 1987). Another unknown is the height of the dykes. The dykes are now exposed between sea level and an elevation of 960 m. Assuming that the volcano was initially 1600 m high, these zones were between 640 and 1600 m beneath the summit. Assuming a magma chamber at 3000 m depth when the dykes were injected, the minimum height of the dykes was greater than 1400 m and their maximum height greater than 2360 m, but there are no clear upper limits (a dyke height potentially greater than the source depth means a dyke that reaches the surface and feeds a lava flow). We simulated two contrasting conditions for the distribution law of dyke height: Ko'olau1 and Ko'olau2. In the first model, Ko'olau1, dyke heights range from 2000 to 2500 m and no dyke reaches the surface. In the second model, Ko'olau2, the range is 4000–5000 m and more than 90% of the dykes reach the surface. The parameters of these two models are reported in Table 6.

The uplift for the first model (Ko'olau1) is 756 m. The bulge is elongated in the direction of the intrusions. Its length is 35 km and its width is 15 km (Fig. 14). The value of the vertical displacement is significantly lower than the estimation of Walker (1987). In the second model, Ko'olau2, the maximum vertical displacement due to the intrusions is 1329 m (Fig. 15a). The length of the deformation parallel to the dykes is 30 km and its width normal to the intrusions is 12 km. In this case, the vertical displacement of the model is similar to the estimate of Walker (1987).

The dykes reaching the surface (93%) feed lava flows the characteristics of which are reported in Table 6. The position of the vent on the dyke trace is chosen at random. The yield strength is not well known and may vary widely, depending on lava temperature and composition. Values reported in the literature vary from a few tens of Pa to 250 kPa (Hulme, 1974; Pinkerton and Wilson, 1994; Shaw et al., 1968). Small values of the yield strength, less than 100 Pa, result in very thin, non-realistic flows. So we used a yield strength range of 5–15 kPa. Individual volumes of the lava flows are based on the data available for Kilauea volcano.

Table 6
Medium, source, dyke and lava-flow parameters used in models Ko'olau1 and Ko'olau2 (Section 5). For the "Gaussian" distribution, see caption of Table 3. For the log-normal law the "minimum" and "maximum" values stand for $x_0 \exp(-2m)$ and $x_0 \exp(2m)$ (cf. Eq. (A14))

Characteristics of the medium	Poisson ratio	0.25	
Characteristics of the source (disc)	Depth (m)	3000	
	Radius (m)	4000	
Characteristics of the dykes	Width (m)	Minimum	0.25
		Maximum	1.25
		Distribution	Log-normal
	Length (m)	Minimum	15 000
		Maximum	20 000
		Distribution	Gaussian
	Height (m)	Minimum (Ko'olau1)	2000
		Maximum (Ko'olau1)	2500
		Minimum (Ko'olau2)	4000
		Maximum (Ko'olau2)	5000
		Distribution	Gaussian
	Dip (°)	Minimum	65
		Maximum	85
		Distribution	Gaussian
	Azimuth (°)	Minimum	85
		Maximum	95
		Distribution	Uniform
Characteristics of the lava flows (Ko'olau2 only)	Volume (10^6 m^3)	Minimum	1
		Maximum	20
		Distribution	Gaussian
	Yield strength (kPa)	Minimum	5
		Maximum	15
		Distribution	Gaussian
	Aspect ratio	Minimum	0.01
		Maximum	0.02
		Distribution	Uniform

Adding the lava flows to the model Ko'olau2 increases its elevation slightly to 1593 m. The mean slope is 6.5° (Fig. 15b). The dykes being very long and the source very large, the contribution of lava flows to edifice height is only 16% although they represent 30% of the edifice volume. This low contribution of lava flows to the construction of the volcano is related to the fact that the mean volume of the lava flows (11×10^6 m^3) is small compared with the mean volume of the intrusions (55×10^6 m^3).

Although our approach is not suited (nor intended) to model the complexity of growth processes of volcanic edifices, our models based on actual observations of the interior of Ko'olau allow us to assess the most probable dominant growth mechanism for this type of edifice.

Well-developed and long volcanic rift zones imply the emplacement of numerous and long dykes. This fact is well illustrated in the case of Ko'olau where exceptional outcrop conditions permit observations of the dyke complex at depth. The models demonstrate that it is the development of the dyke swarm that probably accounts for most of the elevation and shape of the rift zone. Changing the dyke and lava-flow parameters, within ranges realistic for basaltic shields, will not significantly alter our conclusions.

6. Case study 2: Piton de la Fournaise central cone

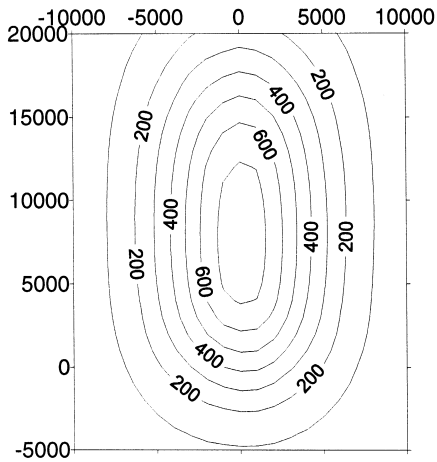The central cone of Piton de la Fournaise volcano is

Fig. 14. Model Ko'olau1: contour map of the deformation induced by 7400 dykes with characteristics as listed in Table 6. Graduations and contour labels in metres.

located within a large caldera-like structure, Enclos Fouqué (Fig. 16). The cone culminates at 2631 m, rises 400 m above the floor of Enclos Fouqué, and has a diameter of about 4 km. Two collapse craters occupy the summit: Bory crater on the west and Dolomieu crater on the east. The cone is slightly elongated E–W and its mean slope of 20° or so is unusually steep for a basaltic shield volcano. It is the present focus of activity of Piton de la Fournaise. During historical times, 95% of the eruption vents were located inside Enclos Fouqué. They are concentrated on the central cone along two rift zones, radiating north and south of the summit, and curving to the NE and SE, respectively, farther from the cone (Lénat, 1988). The other eruptions took place along the rift zones but outside Enclos Fouqué.

The E–W elongation of the cone is in apparent contradiction to the N–S orientation of the rift zones. This fact and the unusually steep slopes suggest that the construction of the cone may have been different from that of typical basaltic shields. Numerical simulations were carried out to investigate the growth processes that could explain the shape of the central cone.

In a first series of tests, we simulate the growth of the cone using parameters available for Piton de la Fournaise or similar volcanoes. The top of the magma chamber has been estimated to lie between 500 and 2000 m beneath the surface and the diameter

of this shallow reservoir is estimated at about 1 km (Lénat et al., 1989; Lénat and Bachèlery, 1990). With most of the vents inside Enclos Fouqué, the dykes are assumed to be shorter than half the diameter of Enclos Fouqué, which is approximately 4 km. The maximum concentration of vents occurs 1 km north and south of Dolomieu crater (Bachèlery, 1986; Lénat, 1988). Assuming that the vents are situated at two thirds of the dyke length, downstream, the mean length of dykes would be 1500 m. Outcropping dykes at Piton de la Fournaise (Grasso and Bachèlery, 1995) have a mean width of 98 cm but the dykes of the central cone could be statistically different in view of its particular morphology. The dykes of the other volcano of Réunion Island, Piton des Neiges (Maillot, 1999), have a mean width of 78.5 cm but they comprise some very thick dykes of evolved composition, the basaltic dykes have a mean width of 56 cm. At Alofau, Pago and Ofu-Olosega volcanoes (Walker and Eyre, 1995) the mean dyke widths are 40, 46 and 51 cm, respectively. At Mt Etna (Compare, 1980) the mean width is 174 cm. At Ko'olau volcano (Walker, 1986, 1987) the mean width is 74.5 cm. Geophysical measurements at Kilauea volcano lead to estimates between 80 and 160 cm (Pollard et al., 1983). The Icelandic dyke swarms (Gudmundsson, 1990, 1995a) are generally thicker (Hvalfjördur: 109 cm, Eastern Iceland: 348 cm, Flateyjarskagi: 535 cm) but the geodynamic context is probably different from that of basaltic shields. A mean width of 75 cm seems to be a realistic starting value for our simulations. Dyke heights are more difficult to constrain. The percentage of the dykes reaching the surface can only be estimated for the monitoring period 1981–1998, during which 29 eruptions and only 5 intrusions not followed by eruptions were observed (unpublished data from the Observatoire Volcanologique du Piton de la Fournaise). This proportion, however, cannot be held as representative of the longer-term behaviour of the volcano, because of probable stress changes with time, as has been observed at Kilauea (e.g. Dzurisin et al., 1984). We opt for dyke heights such that about half the dykes reach the surface. The volume of individual lava flows at Piton de la Fournaise since 1930 (Bachèlery, 1981) follows a log-normal distribution with a median of $3 \times 10^6 \, m^3$. However, some large-volume lava flows were emitted from vents outside Enclos Fouqué or at
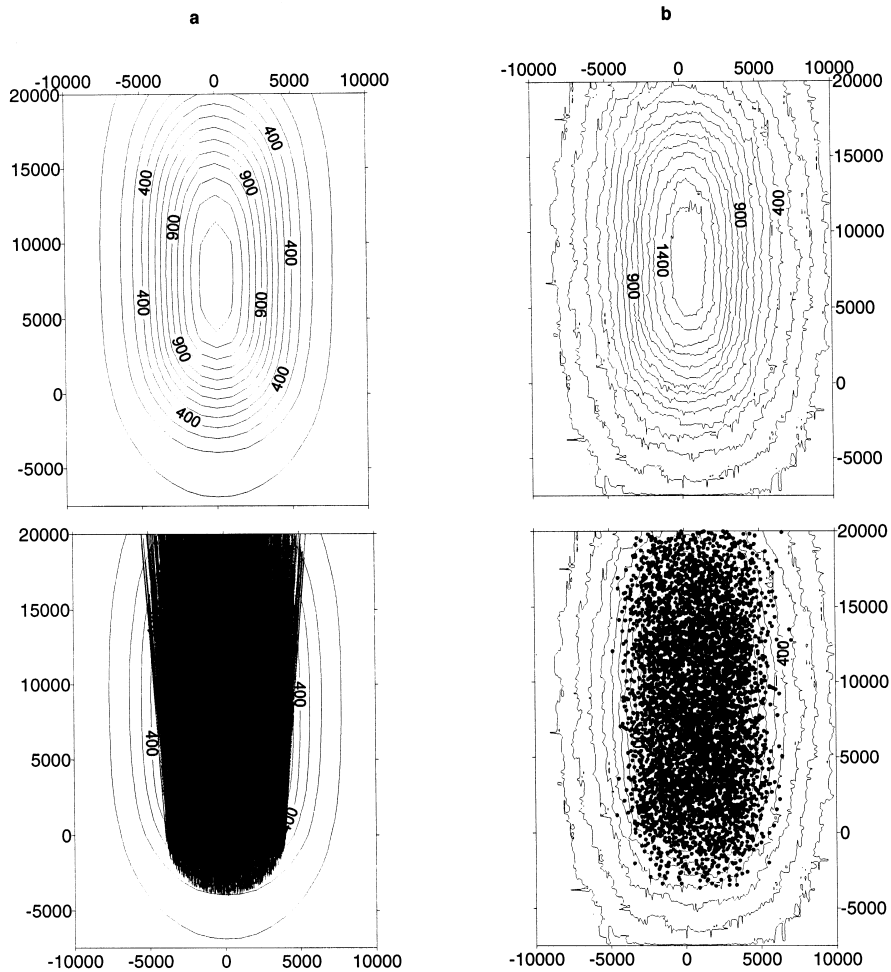
Fig. 15. Model Ko'olau2. (a) Top: contour map of the bulge induced by 7400 non-feeder dykes with characteristics as listed in Table 6; bottom: map of dyke traces (black lines). (b) Top: contour map of the edifice built up by 7400 dykes feeding 6313 lava flows (Table 6); bottom: map of lava vents (black dots). Graduations and contour labels in metres.

least beyond the base of the central cone, so they did not contribute to its construction. A positive-Gaussian volume distribution is therefore preferred in order to avoid very large flows that would bias the computed topography of the central cone. We use the same yield strength range as in model Ko'olau2. Parameters used in the simulation are reported in Table 7 (Fournaise1 model).

Considering a mean time interval between eruptions of 1.5 years and an age of about 5000 years for the cone (Bachèlery, 1981; Gillot et al., 1990), we simulated the intrusion of 3000 dykes which feed 1140 lava flows. The mean thickness of lava flows is 4 m, the mean width

140 m and the mean length 3400 m. The resulting edifice is 290 m high and 9600 m wide, and is elongated in the N–S direction (Fig. 17). It is significantly flatter and wider than the actual cone. This suggests that, in order to obtain a better resemblance between the observed and computed topographies, the model parameters should be modified to simulate shorter or thicker dykes, or a shallower source or shorter lava flows or a combination of those. For example, lava flows tend to flatten the edifice and the number of flows can be reduced by decreasing the dyke heights. Proceeding by trial and error while modifying dykes, source and flow parameters we are led to models that involve a smaller
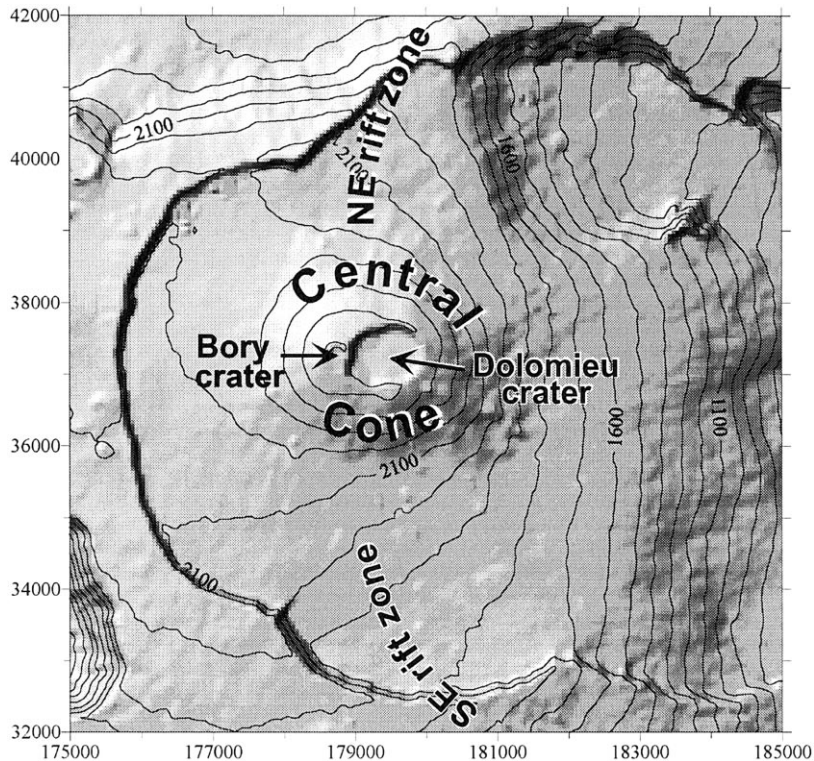
Fig. 16. Shaded relief view of the active zone of Piton de la Fournaise volcano (Réunion Is.). Coordinates in metres (Gauss–Laborde Réunion projection).

and shallower source, shorter and thicker dykes and fewer and shorter lava flows than the first model. For example, Table 8 (Fournaise2 model) shows a set of parameters that produces an edifice comparable to the central cone. This model has a small (100 m) and shallow (500 m) magma chamber, numerous (10 000) very short and thick dykes (mean thickness: 3 m) and infrequent (703) low-volume lava flows. However, whereas the model prediction is good for the E–W profile (Fig. 18a1), it is worse for the N–S (Fig. 18b1) unless we take into account the horizontal displacements. Indeed, we did not take into account the horizontal displacements caused by dyke intrusions for the previous models because we had verified that on large edifices this does not significantly change the topography. Conversely, in the case of a small structure with a very high density of dykes such as the Piton de la Fournaise central cone, this becomes significant. Adding the horizontal displacements to the topography does not significantly change the E–W profile (Fig.

18a3), but it modifies the N–S profile which now better fits the observed one (Fig. 18b3). The cone summit is then slightly elongated E–W. (Fig. 19). In this model, the lava flows contribute only 30% of the edifice volume.

The goal of such modelling is not to fit accurately the virtual to the actual edifices, but to differentiate between processes likely to play a role in the edifice construction. In the case of the central cone of Piton de la Fournaise, our study shows that this unusually steep basaltic cone is probably the result of predominantly endogenous growth through short dykes originating from a small and shallow magma reservoir and of subordinate exogenous growth through low-volume lava flows. The fact that the cone is elongated perpendicular to the main direction of intrusion and vent distribution may be readily explained by the deformation generated predominantly by very short dykes emplaced subparallel to rift-zone trends.

Table 7
Medium, source, dyke and lava-flow parameters used in model Fournaise1. For the "Gaussian" distribution, see caption of Table 3

|			
Characteristics of the medium	Poisson ratio	0.25	
Characteristics of the source (sphere)	Depth (m)	2000	
	Radius (m)	500	
Characteristics of the dykes	Width (m)	Minimum	0.5
		Maximum	1
		Distribution	Gaussian
	Length (m)	Minimum	50
		Maximum	2000
		Distribution	Gaussian
	Height (m)	Minimum	1000
		Maximum	3000
		Distribution	Gaussian
	Dip (°)	Minimum	70
		Maximum	110
		Distribution	Uniform
	Azimuth (°) (northern rift zone)	Minimum	80
		Maximum	100
		Distribution	Uniform
	Azimuth (°) (southern rift zone)	Minimum	260
		Maximum	280
		Distribution	Uniform
Characteristics of the lava flows	Volume (10^6 m^3)	Minimum	1
		Maximum	20
		Distribution	Gaussian
	Yield strength (kPa)	Minimum	5
		Maximum	15
		Distribution	Uniform
	Aspect ratio	Minimum	0.01
		Maximum	0.02
		Distribution	Uniform
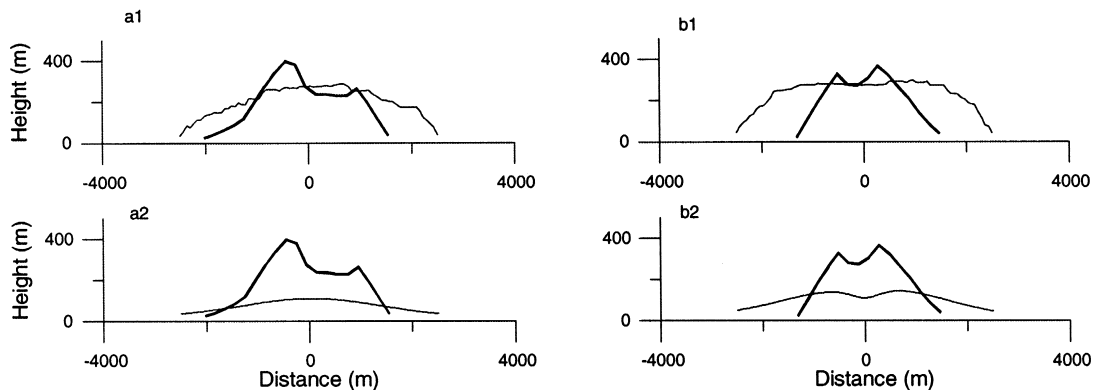
Fig. 17. Model Fournaise1 (3000 dykes and 1140 lava flows, see Table 7). Bold lines: actual profile of the central cone; thin lines: computed profile. (a) E–W profile; (b) N–S profile. (a1,b1) complete modelling (dykes and lava flows); (a2,b2) intrusions only. Vertical exaggeration: 4×.

Table 8
Source, dyke and lava-flow parameters used in model Fournaise2. Only the parameters that differ from model Fournaise1 have been listed; for the other parameters, see Table 7. For the "Gaussian" and log-normal distributions, see captions of Tables 3 and 6

Characteristics of the source (sphere)	Depth (m)		500
	Radius (m)		100
Characteristics of the dykes	Width (m)	Minimum	1
		Maximum	5
		Distribution	Gaussian
	Length (m)	Minimum	1
		Maximum	2000
		Distribution	Log-normal
	Height (m)	Minimum	200
		Maximum	500
		Distribution	Gaussian
Characteristics of the lava flows	Volume (10^6 m^3)	Minimum	0.1
		Maximum	130
		Distribution	Log-normal
	Yield strength (kPa)	Minimum	2.5
		Maximum	10
		Distribution	Uniform

7. Discussion and conclusions

Though based on a simplified approach of dyke and lava-flow statistics, our study demonstrates that the contribution of shallow dyke complexes to the growth of basaltic shields is quantitatively important and that volcanoes should not be considered as mere piles of lava flows. The contribution of each process,
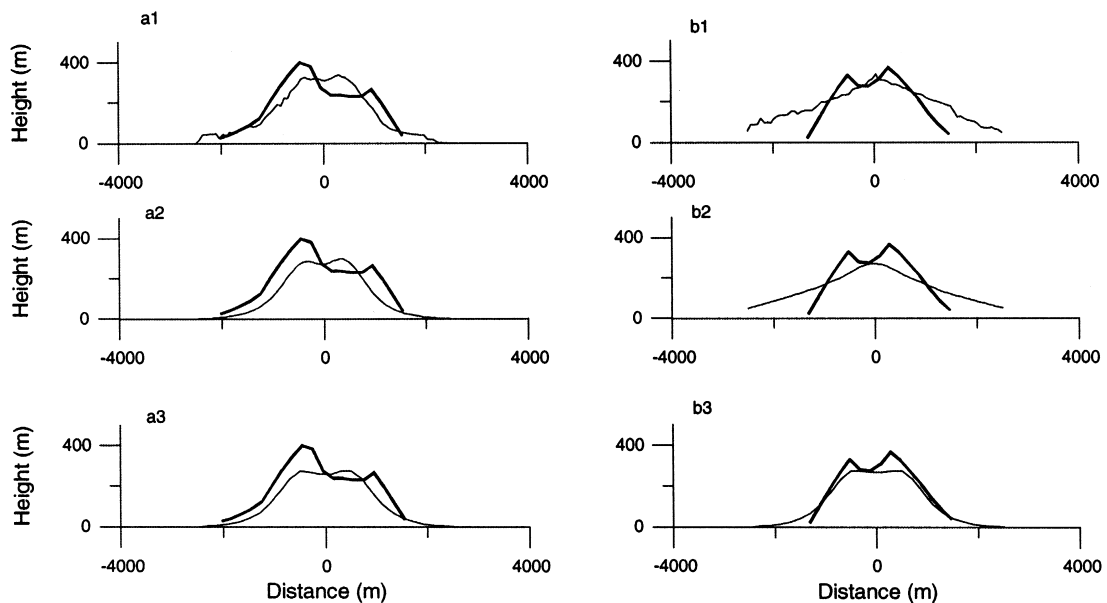

Fig. 18. Model Fournaise2 (10 000 dykes and 703 lava flows, see Table 8). (a1,a2,b1,b2) See caption of Fig. 17. (a3,b3) E–W and N–S profiles when both vertical and horizontal displacements are taken into account (see text). Vertical exaggeration: 4 ×.
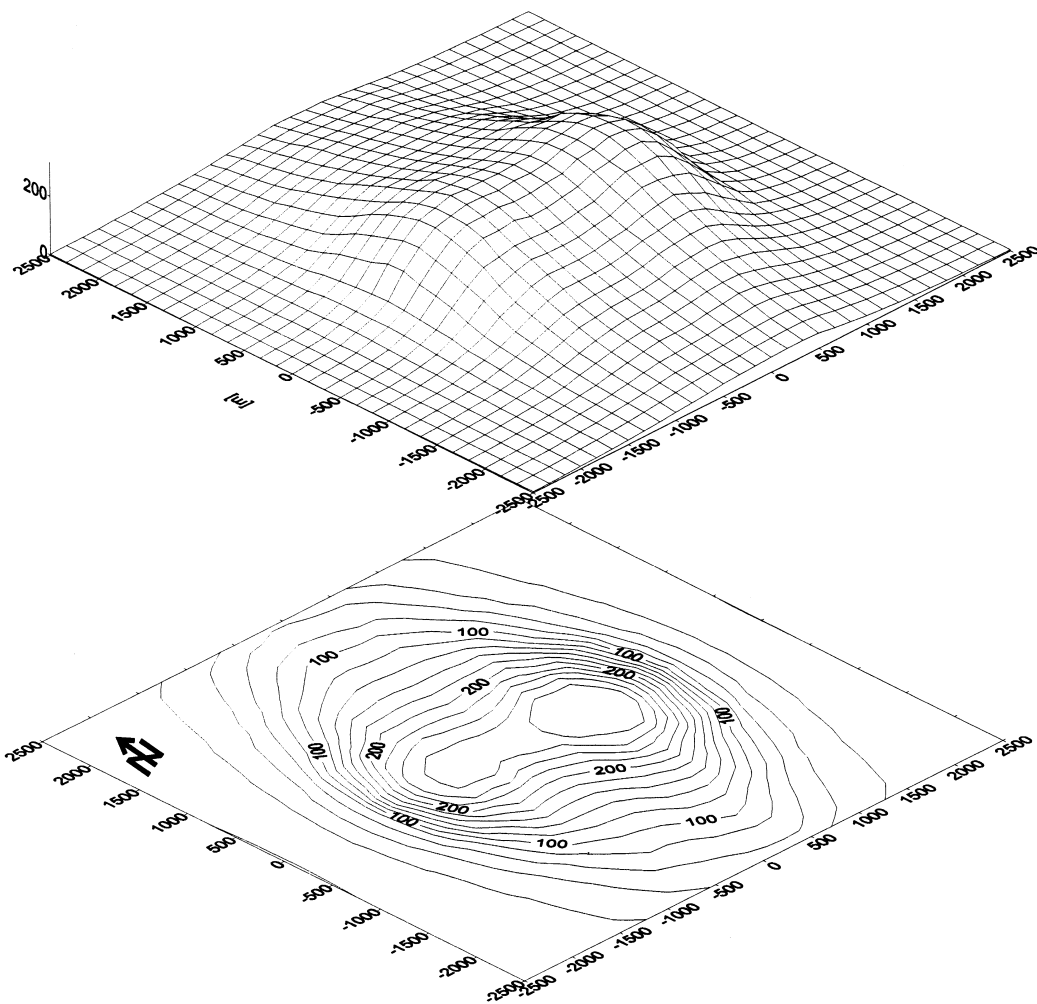
Fig. 19. Model Fournaise2: perspective view and contour map of the deformation (sum of the vertical and horizontal displacements) induced by 10 000 dykes feeding 703 lava flows, with characteristics as listed in Table 8. Graduations and contour labels in metres, vertical exaggeration of the perspective view: 2.5 ×.

endogenous growth and surface growth, depends upon the relative volume of dykes and lava flows. When endogenous growth dominates, thick and short dykes issuing from a small shallow magma chamber will make relatively high edifices with steep slopes. If surface growth dominates, the relative height of the volcano will be a direct function of the yield strength and an inverse function of the individual lava volumes. Even in the case of dominant surface growth, the geometry of the dykes still plays an important role by determining the position of the vents.

Important processes are disregarded by the present model, like cumulates settling in reservoirs, volcaniclastic deposits, gravitational spreading, erosion and other destructive processes. It is therefore better suited to the study of pristine young basaltic volcanoes than composite volcanoes. This is the case of the central

cone of Piton de la Fournaise (Réunion Is.), which is less than 5000 years old. The simulations lead to the inference that its steep flanks and its E–W elongation are strongly impacted by endogenous growth. This suggests that, unlike during the recent years, the long-term number of dyke intrusions significantly exceeds that of eruptions. At Ko'olau volcano (O'ahu Is., Hawai'i) the deformation induced by dykes could be responsible for at least 50% of the estimated original height of the volcano as well as for its general shape. Using dyke geometries as described by Walker (1986, 1987) and lava-flow characteristics similar to those of Kilauea volcano (Hawai'i Is.), we are able to reconstruct an edifice similar to the volcano, with its estimated original height.

A key parameter is the proportion p_{fd} of dykes that reach the surface (feeder dykes). It is related to the proportion p_{er} of volcanic output (extrusive rocks) relative to total magma supply (intrusive and extrusive rocks), though indirectly: eruption-feeder dykes enter the intrusive budget, and the average ratio of lava-flow (and other eruptive products) volume to feeder-dyke volume may vary widely. Both p_{fd} and p_{er} are poorly known but seem to be highly variable. For long periods of igneous activity (thousands to millions of years) the extrusive-rock proportion p_{er} estimated from outcrops lies between 6 and 20% for intracontinental and island-arc settings and between 14 and 25% for oceanic hot spots and ridges (Crisp, 1984). Calculations based on the compared duration of activity and dormancy periods of presently active volcanoes give larger values of p_{er}, up to 56% (Wadge, 1982). Monitoring at Kilauea from 1959 to 1983 led to $p_{fd} = 57\%$ and $p_{er} = 35\%$ (Dzurisin et al., 1984). At Piton de la Fournaise the observed value of p_{fd} was 85% from 1981 to 1998 but small intrusions may have remained undetected. On the other hand, field data on several thousand dykes from Iceland and Tenerife indicate a small value of the feeder-dyke proportion p_{fd} (Gudmundsson, 1999), possibly a few percent or less. At Piton de la Fournaise the morphology of the central cone indicates a mean p_{fd} value of about 7% over 4000 or 5000 years, with p_{er} about 30% (this study). At Ko'olau volcano p_{fd} is not well constrained but p_{er} is less than 35% even when assuming a very conservative value of p_{fd} exceeding 90% for the whole period of volcano building (this study).

The method we have developed can be applied to the study of growth processes of basaltic shields and other volcano types in various environments, including non-terrestrial volcanism. The method can evolve towards a more sophisticated simulation of source geometry, medium rheology, dyke intrusions and lava flow. The model can be further refined by including the computation of internal stresses and their evolution, in order to evaluate the possible occurrence and location of volcanotectonic events, such as flank landslides, an important point for the prevention of volcanic hazards.

Acknowledgements

Appendix A. Simple two-parameter distribution laws

Eqs. (A1)–(A11), (A16) and (A17) below are classical and can be found in many textbooks, e.g. Swan and Sandilands (1995). Numerical methods to get random variables following the various distribution laws can be found in Press et al. (1986). In this study, each dyke or lava-flow characteristic X is considered as a continuous random variable. The probability density function (p.d.f.) f is defined from the probability of getting X within an infinitesimal interval:

$$P[x \leq X \leq x + dx] = f(x)\,dx \qquad (A1)$$

The probability of getting X in some finite interval is thus given by:

$$P[x_1 \leq X \leq x_2] = \int_{x_1}^{x_2} f(x)\,dx \qquad (A2)$$

and, in particular:

$$\int_{-\infty}^{\infty} f(x)\,dx = 1 \tag{A3}$$

The mean value of X is given by:

$$\bar{X} = \int_{-\infty}^{\infty} x f(x)\,dx \tag{A4}$$

and its standard deviation and variance by:

$$\sigma_X = \sqrt{v_X}$$

and $\nu_X = \int_{-\infty}^{\infty} (x - \bar{X})^2 f(x)\,dx = \int_{-\infty}^{\infty} x^2 f(x)\,dx - \bar{X}^2$ $\tag{A5}$

Another important function is the cumulative probability function (c.p.f.) F:

$$F(x) = P[X \geq x] = \int_{x}^{\infty} f(\xi)\,d\xi \tag{A6}$$

which has the following properties:

$$F(-\infty) = 1, \quad F(\infty) = 0 \quad \text{and} \quad f(x) = -\frac{dF}{dx} \tag{A7}$$

The simplest distribution law is the continuous uniform distribution:

$$f(x) = \begin{cases} 0 & \text{if } x < a \\ \dfrac{1}{b-a} & \text{if } a \leq x \leq b \\ 0 & \text{if } x > b \end{cases} \tag{A8}$$

and

$$F(x) = \begin{cases} 1 & \text{if } x \leq a \\ \dfrac{b-x}{b-a} & \text{if } a \leq x \leq b \\ 0 & \text{if } x \geq b \end{cases}$$

for which:

$$\bar{X} = \frac{a+b}{2} \qquad \text{and } \sigma_X = \frac{b-a}{2\sqrt{3}} \tag{A9}$$

In this study this distribution law may be appropriate for dyke strikes (with e.g. $a = 0$ and $b = 2\pi = 360°$).

The most popular distribution law is the Gaussian (or Laplace–Gauss or "normal") law:

$$f(x) = \frac{1}{s\sqrt{2\pi}} \exp\left[-\left(\frac{x-x_0}{s\sqrt{2}}\right)^2\right] \tag{A10}$$

and

$$F(x) = \frac{1}{2}\left[1 - \operatorname{erf}\left(\frac{x-x_0}{s\sqrt{2}}\right)\right]$$

for which:

$$\bar{X} = x_0 \qquad \text{and} \qquad \sigma_X = s \tag{A11}$$

Values should tend to come from this distribution law when they are the sum or the mean of many independent random contributions (central limit theorem). However, most physical or geological characteristics are positive quantities so the Gaussian law should never apply unless $\sigma_X \ll \bar{X}$. We use instead the positive-Gaussian law, which is simply the Gaussian law left-truncated at $x = 0$:

$$f(x) = \begin{cases} 0 & \text{if } x < 0 \\ \dfrac{A}{s\sqrt{2\pi}} \exp\left[-\left(\dfrac{x-x_0}{s\sqrt{2}}\right)^2\right] & \text{if } x \geq 0 \end{cases}$$

with $A = \dfrac{2}{1 + \operatorname{erf}\left(\dfrac{x_0}{s\sqrt{2}}\right)}$ $\tag{A12a}$

and

$$F(x) = \begin{cases} 1 & \text{if } x \leq 0 \\ 1 - \dfrac{A}{2}\left[\operatorname{erf}\left(\dfrac{x_0}{s\sqrt{2}}\right) + \operatorname{erf}\left(\dfrac{x-x_0}{s\sqrt{2}}\right)\right] & \text{if } x \geq 0 \end{cases}$$
$$\tag{A12b}$$

for which:

$$\bar{X} = x_0 + \frac{As}{\sqrt{2\pi}} \exp\left[-\left(\frac{x_0}{s\sqrt{2}}\right)^2\right] \tag{A13}$$

and $\sigma_X = \sqrt{s^2 - \bar{X}(\bar{X} - x_0)}$

A random variable X follows a log-normal (or Galton–MacAlister) law if its logarithm is normally distributed.

This distribution law is characterised by:

$$f(x) = \begin{cases} 0 & \text{if } x \le 0 \\ \dfrac{1}{mx\sqrt{2\pi}} \exp\left[-\dfrac{1}{2m^2}\left(\ln\dfrac{x}{x_0}\right)^2 \right] & \text{if } x > 0 \end{cases}$$

(A14a)

and

$$F(x) = \begin{cases} 1 & \text{if } x \le 0 \\ \dfrac{1}{2}\left[1 - \text{erf}\left(\dfrac{1}{m\sqrt{2}} \ln\dfrac{x}{x_0}\right) \right] & \text{if } x \ge 0 \end{cases}$$

(A14b)

and leads to:

$$\bar{X} = x_0 \exp\left(\dfrac{m^2}{2}\right) \qquad \text{and} \qquad \sigma_X = \bar{X}\sqrt{\exp(m^2) - 1}$$

(A15)

The exponential distribution usually arises when discrete events occur randomly and independently in space or time. If the number of events per unit interval follows a Poisson distribution then the interval between events follows the law defined by:

$$f(x) = \begin{cases} 0 & \text{if } x < 0 \\ \lambda \exp(-\lambda x) & \text{if } x \ge 0 \end{cases}$$

$$\text{and } F(x) = \begin{cases} 1 & \text{if } x \le 0 \\ \exp(-\lambda x) & \text{if } x \ge 0 \end{cases}$$

(A16)

for which:

$$\bar{X} = \sigma_X = \dfrac{1}{\lambda}$$

(A17)

This distribution law has only one parameter. However, it may be that no interval less than a certain cut-off value a is allowed, which leads to the two-parameter truncated exponential law:

$$f(x) = \begin{cases} 0 & \text{if } x < a \\ \lambda \exp[-\lambda(x - a)] & \text{if } x \ge a \end{cases}$$

$$\text{and } F(x) = \begin{cases} 1 & \text{if } x \le a \\ \exp[-\lambda(x - a)] & \text{if } x \ge a \end{cases}$$

(A18)

for which:

$$\bar{X} = a + \dfrac{1}{\lambda} \qquad \text{and } \sigma_X = \dfrac{1}{\lambda}$$

(A19)

The power-law distribution arises in the context of fractality. It is characterised by a c.p.f. proportional to $1/x^m$ where m is a positive constant. The fractal dimension is m if x is a distance, $m/2$ if x is a surface and $m/3$ if x is a volume or mass (Turcotte, 1992). It is clear, however, that the fractal behaviour cannot extend to an arbitrarily small value of x since $F(x)$ cannot diverge when x tends to 0. The left-truncated power-law distribution is characterised by:

$$f(x) = \begin{cases} 0 & \text{if } x < a \\ \dfrac{ma^m}{x^{m+1}} & \text{if } x > a \end{cases}$$

$$\text{and } F(x) = \begin{cases} 1 & \text{if } x \le a \\ \left(\dfrac{a}{x}\right)^m & \text{if } x \ge a \end{cases}$$

(A20)

for which:

$$\bar{X} = \dfrac{m}{m - 1}a \ (\text{if } m > 1)$$

$$\text{and } \sigma_X = \dfrac{a}{m - 1}\sqrt{\dfrac{m}{m - 2}} \ (\text{if } m > 2)$$

(A21)

$\bar{X}$ is infinite for $m \le 1$ and σ_X for $m \le 2$. For most geological and physical characteristics the mean and standard deviation cannot diverge: if data indicate fractality with an exponent m less than 2, the fractal behaviour cannot extend to an arbitrarily high value of x and a power-law distribution both left- and right-truncated should be considered (with three parameters).

References

Bachèlery, P., 1981. Le Piton de la Fournaise (Ile de la Réunion): étude volcanologique, structurale et pétrologique. Thèse de l'Université Clermont-Ferrand II, France, 215 pp.

Bachèlery, P., 1986. Les divers types d'éruptions du Piton de la Fournaise. In: Stieljes (Ed.), Notice explicative de la carte des coulées historiques du Piton de la Fournaise, publication du BRGM, pp. 33–36.

Barca, D., Crisci, G.M., Di Gregorio, S., Nicoletta, F., 1993. Cellular automata methods for modeling lava flows: simulation of the 1986–1987 eruption, Mount Etna, Sicily. In: Kilburn,

C.R.J., Luongo, G. (Eds.), Active Lava Flows. UCL Press, pp. 291–309.

Bonafede, M., Danesi, S., 1997. Near-field modifications of stress induced by dyke injection at shallow depth. Geophys. J. Int. 130, 433–448.

Bonafede, M., Rivalta, E., 1998. The tensile dislocation problem in a layered elastic medium. Geophys. J. Int. 136, 341–356.

Compare, D., 1980. Rapports de mission 1979–1980. Recherches sur les dykes et leur encaissant dans la Valle del Bove à l'Etna (Sicile, Italie). Bull. PIRPSEV 37, 102 pp.

Crisp, J.A., 1984. Rates of magma emplacement and volcanic output. J. Volcanol. Geotherm. Res. 20, 177–211.

Decker, R.W., 1987. Dynamics of Hawaiian volcanoes: an overview. U.S. Geol. Surv. Prof. Pap. 42, 997–1018.

Delaney, P.T., McTigue, D.F., 1994. Volume of magma accumulation or withdrawal estimated from surface uplift or subsidence, with application to the 1960 collapse of Kilauea Volcano. Bull. Volcanol. 56, 417–424.

Dvorak, J., Okamura, A., 1987. Geometry of intrusions and eruptive fissures at Kilauea volcano determined from trilateration measurements. Hawaii Symposium on How Volcanoes Work, Hilo, Hawaii, Abstr. vol., p. 58.

Dzurisin, D., Koyanagi, R.Y., English, T.T., 1984. Magma supply and storage at Kilauea Volcano, Hawaii, 1956–1983. J. Volcanol. Geotherm. Res. 21, 177–206.

Foulger, G.R., Jahn, C.-H., Seeber, G., Einarsson, P., Julian, B.R., Heki, K., 1992. Post-rifting stress relaxation at the divergent plate boundary in Northeast Iceland. Nature 358, 488–490.

Francis, P., Oppenheimer, C., Stevenson, D., 1993. Endogenous growth of persistently active volcanoes. Nature 366, 554–557.

Giberti, G., Jaupart, C., Sartoris, G., 1992. Steady-state operation of Stromboli volcano, Italy: constraints on the feeding system. Bull. Volcanol. 54, 535–541.

Gillot, P.-Y., Nativel, P., Condomines, M., 1990. Géochronologie du Piton de la Fournaise. In: Lénat, J.-F. (Ed.), Le volcanisme de la Réunion (Monographie). pp. 243–253.

Grasso, J.R., Bachèlery, P., 1995. Hierarchical organisation as a diagnostic approach to volcano mechanics: validation on Piton de la Fournaise? Geophys. Res. Lett. 22, 2897–2900.

Gudmundsson, A., 1983. Form and dimensions of dykes in eastern Iceland. Tectonophysics 95, 295–308.

Gudmundsson, A., 1990. Dyke emplacement at divergent plate boundaries. In: Parker, A.J., Rickwood, P.C., Tucker, D.H. (Eds.), Mafic Dykes and Emplacement Mechanisms. Balkema, Rotterdam, pp. 47–62.

Gudmundsson, A., 1995a. Infrastructure and mechanics of volcanic systems in Iceland. J. Volcanol. Geotherm. Res. 64, 1–22.

Gudmundsson, A., 1995b. The geometry and growth of dykes. In: Baer, G., Heimann, A. (Eds.), Physics and Chemistry of Dykes. Balkema, Rotterdam, pp. 23–34.

Gudmundsson, A., 1998. Magma chambers modeled as cavities explain the formation of rift zone central volcanoes and their eruption and intrusion statistics. J. Geophys. Res. 103 (B4), 7401–7412.

Gudmundsson, A., 1999. Injection and arrest of dykes: implications for volcanic hazards. J. Volcanol. Geotherm. Res. 88, 1–13.

Harris, A.J.L., Stevenson, D.S., 1997. Magma budget and steady-state activity of Vulcano and Stromboli. Geophys. Res. Lett. 24, 1043–1046.

Hofton, M.A., Foulger, G.R., 1996a. Postrifting anelastic deformation around the spreading plate boundary, north Iceland. 1. Modeling of the 1987–1992 deformation field using a viscoelastic Earth structure. J. Geophys. Res. 101 (B11), 25 403–25 421.

Hofton, M.A., Foulger, G.R., 1996b. Postrifting anelastic deformation around the spreading plate boundary, north Iceland. 2. Implications of the model derived from the 1987–1992 deformation field. J. Geophys. Res. 101 (B11), 25 423–25 436.

Hulme, G., 1974. The interpretation of lava flow morphology. Geophys. J. R. Astron. Soc. 39, 361–384.

HVO, 2000a. Eruption History of Kilauea Volcano, Hawai'i. USGS Hawaiian Volcano Observatory web site, http://hvo.wr.usgs.-gov/kilauea/history/historytable.html.

HVO, 2000b. Eruption History of Mauna Loa Volcano, Hawai'i. USGS Hawaiian Volcano Observatory web site, http://wwwhvo.wr.usgs.gov/maunaloa/history/historytable.html.

Ishihara, K., Iguchi, M., Kamo, K., 1990. Numerical simulation of lava flows on some volcanoes in Japan. In: Fink, J.H. (Ed.), Lava Flows and Domes. Springer, Berlin, pp. 174–207.

Jackson, D.B., Swanson, D.A., Koyanagi, R.Y., Wright, T.L., 1975. The August and October 1968 east rift eruptions of Kilauea volcano, Hawaii. U.S. Geol. Surv. Prof. Pap. 890, 33 pp.

Lénat, J.-F., 1988. Patterns of volcanic activity of Piton de la Fournaise (Réunion Island, Indian Ocean). A synthesis based on monitoring data between 1980 and July 1985, and on historic records since 1930. In: Latter, J.H. (Ed.), Volcanic Hazards: Assessment and Monitoring. IAVCEI Proceedings in Volcanology, vol. 1. Springer, Berlin, pp. 312–338.

Lénat, J.-F., Bachèlery, P., 1990. Structure et fonctionnement de la zone centrale du Piton de la Fournaise. In: Lénat, J.-F. (Ed.), Le volcanisme de la Réunion (Monographie). pp. 257–296.

Lénat, J.-F., Bachèlery, P., Bonneville, A., Hirn, A., 1989. The beginning of the 1985–1987 eruptive cycle at Piton de la Fournaise (La Réunion): new insights in the magmatic and volcano-tectonic systems. J. Volcanol. Geotherm. Res. 36, 209–232.

Lockwood, J.P., Lipman, P.W., 1987. Holocene eruptive history of Mauna Loa volcano. In: Decker, R.W., Wright, T.L, Stauffer, P.H. (Eds.), Volcanism in Hawaii. U.S. Geol. Surv. Prof. Pap. 1350, 509–535.

Macdonald, G.A., Abbott, A.T., Peterson, F.L., 1986. Volcanoes in the sea: the geology of Hawaii, 2nd ed. University of Hawaii Press, Honolulu, 517 pp.

Maillot, E., 1999. Les systèmes intrusifs des volcans boucliers océaniques, Ile de la Réunion (Océan Indien): approche structurale et expérimentale. Thèse de l'Université de la Réunion, 289 pp.

Middleton, G.V., Wilcock, P.R., 1994. Mechanics in the Earth and Environmental Sciences. Cambridge University Press, Cambridge, 459 pp.

Mogi, K., 1958. Relations between the eruptions of various volcanoes and the deformations of the ground surface around them. Bull. Earthquake Res. Inst. 36, 99–134.

Okada, Y., 1985. Surface deformation due to shear and tensile faults in a half-space. Bull. Seismol. Soc. Am. 75, 1135–1154.

Pinkerton, H., Wilson, L., 1994. Factors controlling the length of channel-fed lava flows. Bull. Volcanol. 56, 108–120.

Pollard, D.D., Delaney, P.T., Duffield, W.A., Endo, E.T., Okamura, A.T., 1983. Surface deformation in volcanic rift zones. Tectonophysics 94, 541–584.

Press, W.H., Flannery, B.P., Teukolsky, S.A., Vetterling, W.T., 1986. Numerical Recipes: The Art of Scientific Computing. Cambridge University Press, Cambridge, 818 pp.

Romano, R., Sturiale, C., 1982. The historical eruptions of Mt. Etna (volcanological data). Mem. Soc. Geol. Ital., 75–97.

Ryan, M.P., 1987. Elasticity and contractancy of hawaiian olivine tholeiite and its role in the stability and structural evolution of subcaldera magma reservoirs and rift systems. In: Volcanism in Hawaii. U.S. Geol. Surv. Prof. Pap. 1350, 1395–1447.

Shaw, H.R., Wright, T.L., Peck, D.L., Okamura, R., 1968. The viscosity of basaltic magma: an analysis of field measurement in Makaopuhi lava lake, Hawaii. Am. J. Sci. 266, 225–264.

Swan, A.R.H., Sandilands, M., 1995. Introduction to geological data analysis. Blackwell Science, Oxford, 446 pp.

Swanson, D.A., Duffield, D.A., Fiske, R.S., 1976. Displacement of the south flank of Kilauea volcano: the result of forceful intrusion of magma into the rift zones. U.S. Geol. Surv. Prof. Pap. 963, 1–39.

Takada, A., 1988. Subvolcanic structure of the central dyke swarm associated with the ring complexes in the Shitara district, central Japan. Bull. Volcanol. 50, 106–118.

Turcotte, D.L., 1992. Fractal and chaos in geology and geophysics. Cambridge University Press, Cambridge, 221 pp.

Wadge, G., 1982. Steady state volcanism: evidence from eruption histories of polygenetic volcanoes. J. Geophys. Res. 87, 4035–4049.

Walker, G.P.L., 1973. The lengths of lava flows. Philos. Trans. R. Soc. Lond. A 274, 107–118.

Walker, G.P.L., 1986. Koolau dyke complex, Oahu: intensity and origin of a sheeted-dyke complex high in a Hawaiian volcanic edifice. Geology 14, 310–313.

Walker, G.P.L., 1987. The dike complex of Koolau volcano, Oahu: internal structure of a Hawaiian rift zone. U.S. Geol. Surv. Prof. Pap. 1350, pp. 961–993.

Walker, G.P.L., 1988. Three Hawaiian calderas: an origin through loading by shallow intrusions? J. Geophys. Res. 93 (B12), 14 773–14 784.

Walker, G.P.L., 1992. "Coherent intrusion complexes" in large basaltic volcanoes — a new structural model. J. Volcanol. Geotherm. Res. 50, 41–54.

Walker, G.P.L., 1999. Volcanic rift zones and their intrusion swarms. J. Volcanol. Geotherm. Res. 94, 21–34.

Walker, G.P.L., Eyre, P.R., 1995. Dike complexes in American Samoa. J. Volcanol. Geotherm. Res. 69, 241–254.

Walker, G.P.L., Eyre, P.R., Spengler, S.R., Knight, M.D., Kennedy, K., 1995. Congruent dyke-widths in large basaltic volcanoes. In: Baer, G., Heimann, A. (Eds.), Physics and Chemistry of Dykes. Balkema, Rotterdam, pp. 35–40.

Yang, X.-M., Davis, P.M., 1986. Deformation due to a rectangular tension crack in an elastic half-space. Bull. Seismol. Soc. Am. 76, 865–881.

Young, P., Wadge, G., 1990. Flow front simulation of lava flow. Comput. Geosci. 16, 1171–1191.